Analysis of Broad-Band Echosounder Data Over a Gassy Seabed

F. A. Boyle*, N. P. Chotiros*, N. G. Pace**, O. Bergem**, E. Pouliquen**

*Applied Research Laboratories
The Unversity of Texas at Austin
P. O. Box 8029, Austin TX 78713-8029
Email: boyle@arlut.utexas.edu

**SACLANT Undersea Research Centre
Viale San Bartolomeo, 400
19138 La Spezia, ITALY

Abstract

Calibrated echosoundings from a well-characterized gassy seabed were examined. Acoustic reflection was significantly higher than expected. It is hypothesized that gas bubbles are responsible. Anomalously high levels of reflection appear at the edge of the spectral peak, possibly associated with nonlinear conversion of acoustic energy. An acoustic colormapping method was applied to the data, clearly showing its spectral character. The spectral features appear to carry relevant information about sediment interface roughness and gas content.

1. Introduction

Over the past several decades there has been considerable interest in the physics of sound penetration into the seabed. Much of this work has been driven by a need for reliable mine detection capability.

In 1993, Chotiros et.al. [1] compared the results of normal incidence echosoundings with expectations, based in current acoustic theories. It was found that sandy sediments generally had reflection coefficients that were most consistent with poroelastic modeling. These findings were consistent with previous acoustic penetration experiments [2], in which anomalous acoustic penetration was observed that is explainable via poroelastic theory. The reflection coefficient, in general, was found to have sensitive dependence on the sediment type, suggesting that it might be useful for determining seabed acoustic mechanisms.

A significant problem in seabed acoustics is the question of trapped gas bubbles. Gas bubbles are known to possess strong resonances; in water a bubble in resonance typically has an acoustic scattering cross section 1000 times its geometric cross section [3]. If bubbles are present, even in very small quantities, they can produce strong echoes that are indistinguishable from echoes from rigid objects like rocks. In order to understand the physics of acoustic interaction with the seabed, and the relevance of reflection coefficient measurements, calibrated acoustic data over well-characterized sediments is needed. Unfortunately at present, the database is quite sparse. The subject of this paper is the analysis of one such set of data, collected over a gassy sediment site near Viareggio, Italy in March 1996.

Section 2 contains a description of the data acquisition system. In section 3, the computation of reflection coefficients from the data is explained. Section 4 is a consideration of the ping to ping variability of the bottom echo. In section 5, possible evidence for nonlinear behavior is discussed. Section 6 describes a method of imaging the data to reveal spectral features by mapping the acoustic spectrum into colors. Conclusions are discussed in section 7.

2. Data Description

Acoustic data was collected as illustrated in Fig. 1. Broad band echosoundings were collected by an EG&G UNIBOOM echosounding system, which features an impulsive source, operating over a nominal band between 1

and 15 kHz, with a source level of 208 dB. The source was floated in the water column, with its beam directed downward at normal incidence toward the seabed. A hydrophone was suspended in the water column at a depth of 8 m directly underneath. Each ping recording included a direct acoustic signal from the projector, followed by its reflection from the seabed. Care was taken not to clip the signals, so that the direct arrival could be used for calibration.

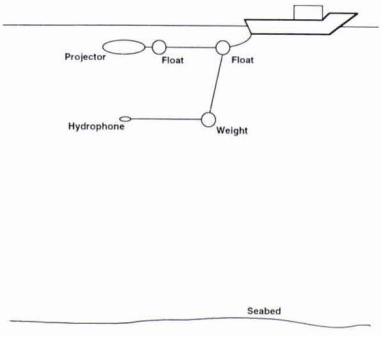

Figure 1: UNIBOOM echosounder configuration

2854 pings of data were collected over a 15 km track, depicted in Fig. 2. The water's depth was 23 m. The track passed over a previously charted front of trapped gas. The seabed consisted of soft sediment, with a mean grain size, determined from sediment grab samples, ranging from 3.8 to 5.3 ϕ, where ϕ is a logarithmic measure of grain size defined as follows:

$$2^{-\phi} = \text{grain diameter in mm}$$

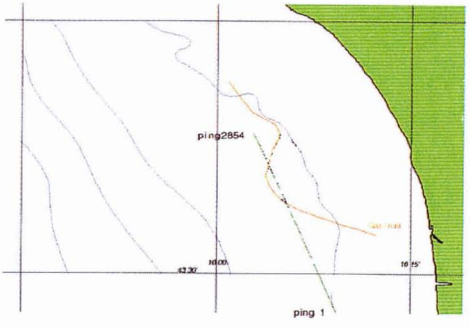

Figure 2: Track over experiment site

Fig. 3 is a waterfall recording of the whole set of pings. The first return, at 6 ms, is the direct arrival of the acoustic signal from the projector to the hydrophone. This is followed, at 30 ms by the bottom bounce. In general, the reflection consists of a bright interface return, followed by features from the sub-bottom that are horizontally stratified. In several locations there are vertical features, believed to be associated with gas bubbles percolating upward through the sediment column. Toward the end of the run is a very dominant example of such a feature, likely associated with the gas front.

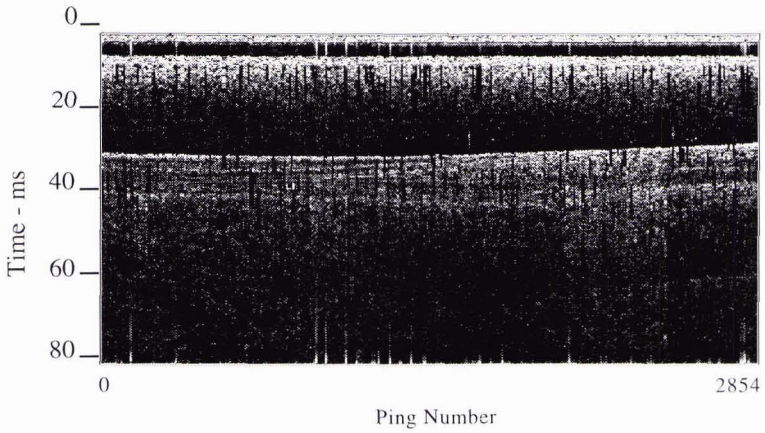

Figure 3: Waterfall plot of recorded data over track

3. Computation of Reflection Coefficient

By comparing the direct arrival with the initial portion of the bottom bounced signal, not including sub-bottom returns, a determination is made of the seabed's reflection coefficient. This calculation is summarized in Figure 4, for a single representative ping. Fig. 4a is an example of the raw time series. In Figure 4b, a linear time varying gain is applied to the signal to compensate for spherical spreading. This method of compensating for spreading insures that the correct spreading loss factor is used for each ping, even when the depth and source-to-receiver distance vary between pings. Apparent in Fig. 4b are the direct signal at 6 ms, followed by the bottom echo at 30 ms, and at 38 ms by a bottom-surface echo. Higher order bottom-surface interactions are obscured by noise. In Figures 4c and 4d, narrow windows are applied to the signal about each arrival, direct and bottom-reflected. This isolates the bottom echo from features within the sub-bottom. The windows applied in Figs. 4c and 4d were tapered, had a length of 2 ms, and were centered about the amplitude peak of each arrival. The window length was designed to encompassed most of the energy in the direct arrival.

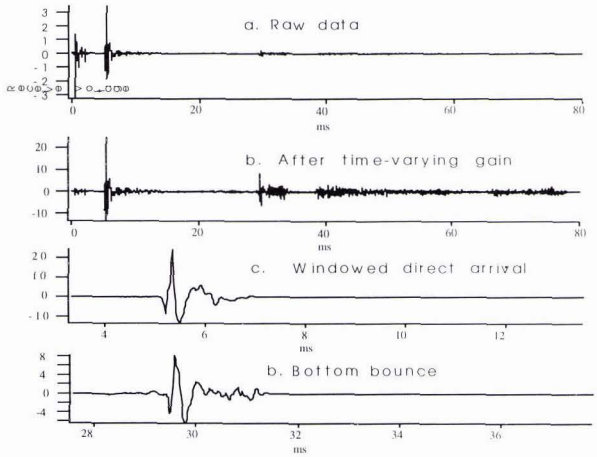

Figure 4: Processing of a single ping to compute reflection coefficient (ping1500)

In general, a bottom echo has two components; a coherent reflection and an incoherent scattered return. The bottom echo depicted in Fig. 4d is very similar in shape to the incident signal of Fig. 4c. This apparent preservation of waveform shape was generally observed in all the pings over the track, and implies that the bottom is acting primarily as a coherent reflector of sound. Acoustic modeling of the site [4], based on the available information about grain size and interface roughness, is consistent; reflection from the bottom is expected to dominate roughness backscatter for frequencies lower than 5 kHz, where most of the acoustic energy is concentrated. It is therefore assumed that the windowed signal in Fig. 4d is predominantly a coherent bottom reflection. This assumption enables an estimate of the reflection coefficient from Figs. 4c and 4d.

The squares of the signals of figs. 4c and 4d are proportional to the energies carried by each wavefront. Since spherical spreading has already been compensated for via the time-varying gain in Fig. 4b, and since absorption in the water column is negligible, the reflection coefficient R can be expressed as a ratio of the energies carried by each of the windowed returns,

$$R = 10log\left(\frac{\int (s_2)^2\, dt}{\int (s_1)^2\, dt}\right),$$

where s_1 and s_2 are windowed direct and bottom-reflected time-series signals depicted in Figs. 4c and 4d. The reflection coefficient is plotted for all pings in Figure 5.

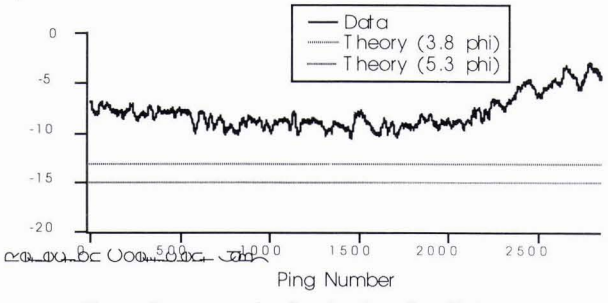

Figure 5: computed reflection loss for all pings

For comparison, theoretical predictions of the reflection coefficient, based on poroelastic modeling of sediments with mean grain sizes of 3.8 and 5.3 phi, are plotted alongside. The theoretical predictions are based on water-saturated sediments with no trapped gas. It is hypothesized that trapped gas bubbles are responsible for the difference between these predictions and the measurement. The measured reflection amplitude is highest toward the end of the track where, visually from the waterfall plot, trapped gas appears to be most prevalent.

The power spectra of the direct and bottom-bounce arrivals can be computed from the Fourier transforms of the windowed signals depicted in Figs. 4c and 4d. They are depicted in Fig. 6, along with their difference in dB, which is the frequency-dependent reflection coefficient.

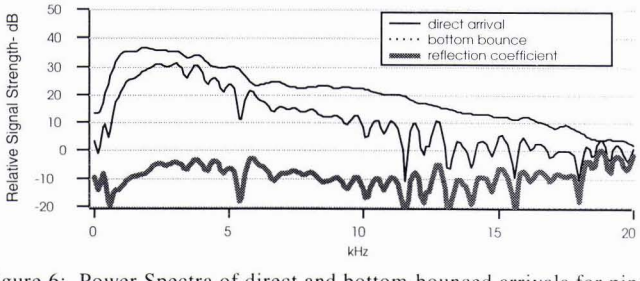

Figure 6: Power Spectra of direct and bottom-bounced arrivals for ping 1500

4. Ping to Ping Variability

There is considerable variability in the reflection coefficient from ping to ping, as is illustrated in Fig. 7, where the reflection coefficient spectra for 20 successive pings are overlaid. At frequencies above 10 kHz, where very little energy is transmitted, the variability is greatest. An explanation for this variability [5], involves interface roughness. A randomly rough bottom can be regarded as a collection of facets, some of which return sound to the sonar while others scatter sound away. Each bottom echo is a coherent sum of contributions from facets that are appropriately aligned. When the position of the sonar platform changes between pings, a different random set of facets will contribute, causing variability in the amplitude of the return.

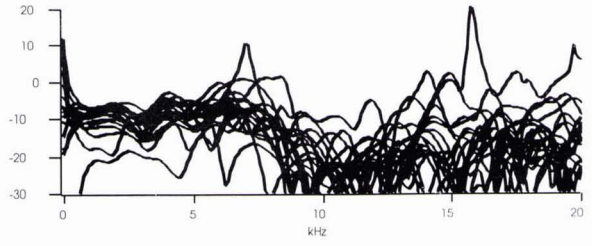

Figure 7: Reflection spectra of 20 successive pings

5. Evidence of Possible Nonlinear Behavior

The evolution of the reflection coefficient spectrum over the whole track is shown in Fig. 8. Although the ping to ping variability across the track is significant, there are clear trends in the reflection spectra. Consistent with Fig. 5, the spectral amplitude is highest near the end of the track where sediment gas is most prevalent. In this region the greatest reflection amplitude occurs between 5 and 10 kHz; frequencies significantly higher than the spectral peak of the incident wave. At these frequencies the reflection coefficients appear to be anomalously high and sometimes approach 0 dB.

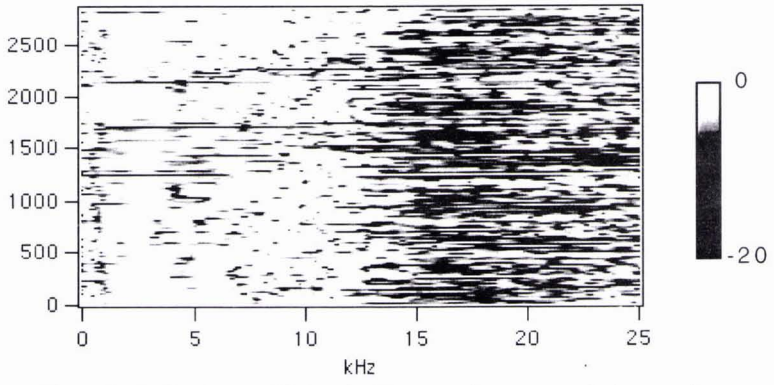

Figure 8: Reflection coefficient in dB versus frequency and ping number

Fig.9 is a comparison of power spectra over two different portions of the track. In each case an average of 50 sequential pings is considered, to offset the effects of ping to ping variability. Fig. 9a involves data taken from the middle of the track, while Fig. 9b is taken from the latter portion of the run, where trapped gas is more likely to prevail. In the former case, the reflection coefficient varies between -19 and -6 dB across the band, while in the latter, the reflection coefficient is as high as +1 dB between about 4 and 7 kHz.

At first glance this appears to suggest that, at some frequencies, more energy is returning than was incident upon the bottom. One hypothesis for this apparent amplification of sound at some frequencies is that the bottom is interacting nonlinearly with the incident sound. Sound that is incident at frequencies between 2 and 3 kHz, for example, may be scattered at second harmonic frequencies, between 4 and 6 kHz. The net effect of this would

be an upshift of acoustic energy toward higher frequencies, elevating the apparent reflection coefficient at higher frequencies at the expense of the lower frequencies. It is well known that bubbly media are highly nonlinear. Nonlinear conversion of acoustic energy by a gassy marine sediment was observed by Karpov, et.al.[6].

It is relevant that the frequency range of the anomaly is higher than the spectral peak for the incident signal. Most of the incident sound from the UNIBOOM is between 1.5 and 4 kHz. Second harmonic frequencies would range between 3 and 8 kHz, which is consistent with the band of the anomalously high reflection levels.

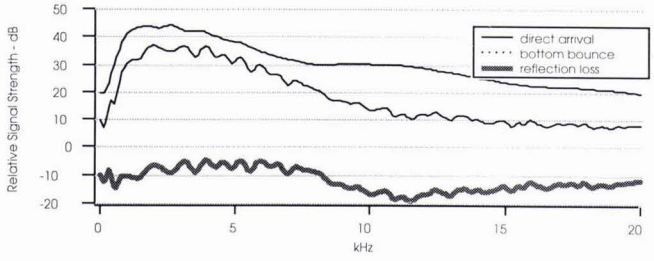

a. average over pings 1500-1550

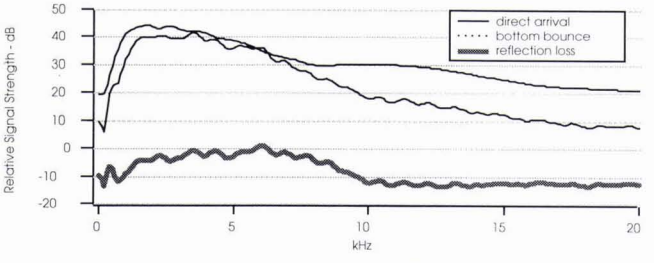

b. average over pings 2750-2800

Figure 9: 50 ping average reflection spectra from middle and final portions of track

6. Colormapping

An acoustic colormapping technique [7] was applied to the data. The method is illustrated in Fig. 10. It is biologically inspired and mimics the eye's treatment of optical signals. The acoustic data is passed, in parallel, through 3 different band-pass filters and the resulting signals displayed via the red, green, and blue pixel elements on a monitor.

In the colormapped display of the Viareggio data, clear spectral features emerge. These include a light gray echo from the water-sediment interface, followed by strata from the sub-bottom with various shades of color. These features appear to convey information about the structure of the seabed.

The light gray leading echo may give an indication about the interface roughness. As was previously stated, the initial echo from the bottom will possess two components; a coherent component and an incoherent one. The coherent component is the portion of sound that is reflected from the water-sediment boundary, while the incoherent component is the part that is scattered by the interface roughness. When the wavelength of the incident signal is large in comparison with the RMS roughness of the ensonified patch, the coherent part will dominate, whereas when the wavelength is relatively small, the incoherent part will dominate. If the band of the incident wave is wide enough to include wavelengths much greater and much less than the RMS interface roughness, the longer (reflected) wavelengths will return with stronger amplitude than the shorter (scattered) ones. In this case, the colormapped leading edge of the bottom return will appear red-enhanced.

The fact that the interface return in the Viareggio data has the same hue as the direct signal may indicate that the RMS roughness is not comparable to wavelengths contained in the incident signal. The colormapping in Fig. 10 was applied between 1500 and 8000 Hz , from 1/2 maximum of the lowest colormapping filter to 1/2 maximum of the highest. This corresponds to wavelengths between 100 cm and 18.75 cm. A bottom that is smooth to within 1/4 of the smallest wavelength, or 4.7 cm, will produce a reflected signal across the band,

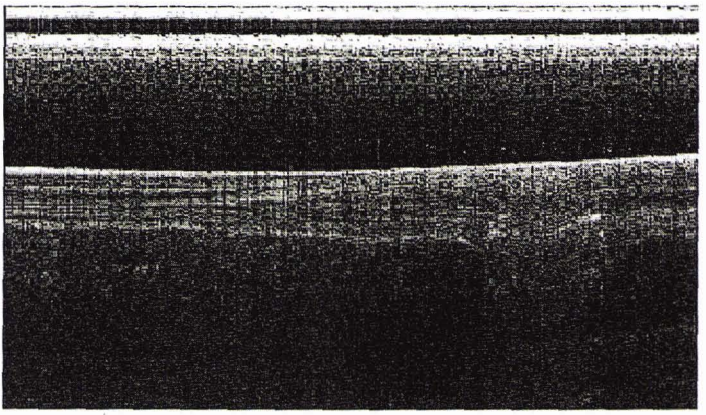

greyscale image of Uniboom data

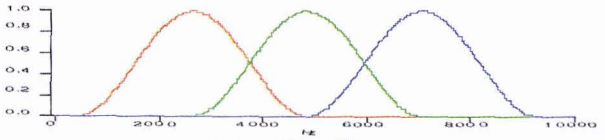

colormapping filters

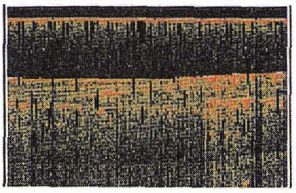

red filtered image

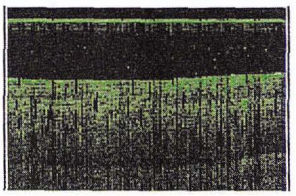

green filtered image

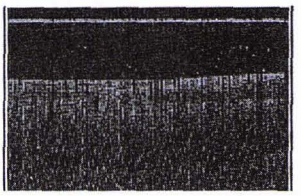

blue filtered image

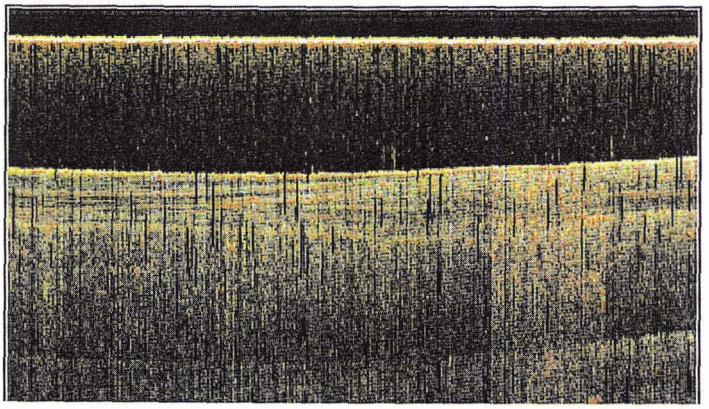

colormapped image

Figure 10: Colormapping of Viareggio data

without significant scattering. The fact that bottom interaction in the Viareggio data does not appear to influence the spectrum may therefore imply that the bottom is smooth to within 4.7 cm. This agrees qualitatively with photographs that were taken of the site. This is also consistent the assumption in section (3) that most of the sound from the interface was reflected rather than scattered.

One possible explanation for the colored strata from the sub-bottom is that they involve layers of trapped gas bubbles with varying size distributions. The colors may indicate the bubbles' resonance frequencies, which depend on their sizes [3]. The color red in the colormap of Fig.10 corresponds to bubbles with resonance frequencies between 1500 and 3500 kHz. For bubbles surrounded by water at sea level, this would correspond to diameters between 4.3 and 1.9 mm. Similarly, "green" bubbles range between 1.9 and 1.2 mm while "blue" bubbles range between 1.2 and 0.9 mm in diameter. The vertical features in the data, where upward migration of sediment gas is apparent, appear to be red-enhanced. This is consistent with the presence of larger bubbles, resonating at lower frequencies, percolating upward through the sediment column. At present this hypothesis is consistent with the data, but not positively conclusive. Other possible interpretations for the colormapped structures might involve coherent effects between boundaries. Further experimentation and analysis is needed.

7. Conclusions

Acoustic data from a gassy site strongly suggests that acoustic bubble interactions account for a significant portion of the sound returned. Anomalously high levels of acoustic reflection appear to be explainable via gas bubble interactions. The spectral content of the return suggests the existence of nonlinearities, possibly caused by gas bubbles.

A colormapping technique yields features that are consistent with scattering from interface roughness and from trapped bubbles. It is possible that the method might be used to obtain quantitative estimates of both. Further research is required.

References

[1] N. P. Chotiros, "Inversion and sandy ocean sediments," *in Modern Approaches in Geophysics*, Vol. XII, Kluwer, Dordrecht, 1995

[2] N. P. Chotiros, "Biot model of sound propagation in water-saturated sand," JASA 97(1), 199-214 (1994)

[3] H. Medwin, "Counting bubbles acoustically, a review," Ultrasonics 15(1) 7-13 (1977)

[4] F. A. Boyle and N. P. Chotiros, "Bottom Grain Gas and Roughness Version 3.0 Bottom Backscatter Model User's Guide," Applied Research Laboratories Technical Report No. 96-10 (1996)

[5] N. P. Chotiros, "Reflection and reverberation in normal-incidence echosounding," JASA 96(5), 2921-2929 (1994)

[6] S. V. Karpov, Z. Klusek, A. L. Matveev, A. I. Popatov, and A. M. Sutin, "Nonlinear Interaction of Acoustic Waves in Gas- saturated Marine Sediments," Acoustical Physics, 42 (4) 464-470 (1996)

[7] F. A. Boyle and N. P. Chotiros, "Mapping acoustic echosounder data to human color vision," JASA 99(4), Pt. 2, 2553 (1996)